

# Cyclin Dependent Kinase 2 Inhibitors an Artificial Neural Network Regression QSAR Study

Claudiu N. Lungu\*

Department of Chemistry, Faculty of Chemistry and Chemical Engineering, Babes-Bolyai University, Arany Janos Str. 11, 400028, Cluj, Romania

\*Corresponding author: Claudiu N. Lungu, Department of Chemistry, Faculty of Chemistry and Chemical Engineering, Babes-Bolyai University, Arany Janos Str. 11, 400028, Cluj, Romania, Tel: +40-742255099; E-mail: lunguclaudiu5555@gmail.com

Received date: February 28, 2018; Accepted date: March 14, 2018; Published date: March 23, 2018

Copyright: © 2018 Lungu CN. This is an open-access article distributed under the terms of the Creative Commons Attribution License, which permits unrestricted use, distribution, and reproduction in any medium, provided the original author and source are credited.

## Abstract

Cyclin dependent kinase (CDK) plays a major role in regulating the cell dynamic. Kinases are present in all known eukaryotes and their regulatory function pathway was evolutionary conserved, suggesting this pathway plays a dominant role in cell growth control and its disruption may result in cell death. Three-dimensional quantitative structure-activity relationships (3D-QSAR), molecular docking and molecular dynamics (MD) simulation strategies were applied to investigate the molecular interaction between active ligands and cyclin dependent kinase 2 (CDK2). A QSAR model was computed using artificial neural network (ANN) regression, with a good predictive ability in internal and external validation. Results were compared with the prototype inhibitor of CDK, Staurosporine. A mixed analysis embodying the QSAR model, molecular docking and molecular dynamics, enabled the pharmacophore high definition. Data provided by MD were highly consistent with the findings of 3D-QSAR model.

**Keywords:** 3D-QSAR; Low molecular dynamics simulation; Conformational analysis; Molecular docking; CDK2 inhibitors; Staurosporine

## Introduction

Screening a large domain of chemical space for a certain compound shape proved to be a valuable tool in identifying compounds with no evident structural similarity but with affinity for the same binding site of a proteic structure. Compounds resulted after such a process can, by functionalization and derivatization, be “shaped” to mimic structural similarity, thus becoming, by the QSAR paradigm, same or, hopefully, better bioactive, or enhanced in drug-like properties. A QSAR model can be used first to find a representative compound in a data set used to build the model. This compound looked at as the least common multiple (i.e., common pharmacophore) can further be used as a lead structure in similar shape screening. The dissociation constant  $K_d$  of the complex ligand-protein can be predicted by the QSAR model. It is also possible that one structure to act on multiple receptors, or to interact with multiple binding sites, located on the same or distinct molecules, such as Staurosporine, able to inhibit protein kinases of different types. Staurosporine (antibiotic AM-2282 or STS) was first isolated in *Streptomyces Staurosporeus*.

Its main biological activity is the competitive binding to protein kinase, against ATP, being a model of ATP competitive kinase inhibitor; however, its great affinity for many CDKs, in other words, its lack of specificity, prevented Staurosporine from clinical use [1]. Despite the progress in discovering more drug-like inhibitors of CDK2, there is still some chemical space available for potent and selective inhibitors of CDK2. Difficulties lie in achieving isomorphous specificity [2], targeting to specific cells or tissues and ensuring correct degree of inhibition [3]. So far, the interaction between CDK2 and ligands is not completely understood, and related mechanism not yet explained. The large variation in binding affinities of these compounds with CDK2 and the relation of biological activity with the flap motion of the

enzyme, as well as, with conformational changes in the catalytic site of CDK2, were investigated using a combined approach including docking and molecular dynamics simulations. The activity data were retrieved from an original series of 264 compounds [4], obtained by isothermal titration calorimetry [5] (ITC) against CDK2; compound structures were curated as follows: only highly active compounds were considered, with  $K_d < 10.000$  nM; structural isomers were not considered. Following these steps, 26 final compounds resulted. The above selection was done for obtaining a model based on non-congeneric compounds in order to expand the chemical space; however, the inactive compounds were not considered in the construction of the model. CDK molecules contain a Walker A motif [6] or a P loop associated with a phosphate group. The Walker a motif is present in ATP and GTP binding proteins. The manner of how this loop is important in binding a compound and is investigated in this study.

## Methods

A data set of 26 molecules with measured  $K_d$ (nM) on human cyclin dependent kinase 2 were used to compute a QASR model by ANN regression method. Target variable was set as  $K_d$ (nM). Dependent variables were as follows: potential energy (kcal/mol), molecular weight (MW), AlogP, polar surface area (PSA), molecular radius (MR), molecular polarity, first Zagreb index (ZI1) [7], Wiener index [8], Xu index [9], Gutman topological descriptor (GTM=ZI2) [10], Eccentricity (ECC) [11], Lipinski's rule of five values [12], and also total connectivity index. Docking study was performed using AutoDock package [13]. 1QA1 PDB id was chosen as a model for CDK2 receptor. Docking site was retrieved from literature and from the model mentioned above [14]. Furthermore, the structure was prepared by the Protein Preparation Wizard in the Schrödinger software suite, including hydrogen atoms, correcting partial charges using the OPLS\_2005 force field and generate protonation states, and in vacuum structure energy minimization. Co-crystal ligand was removed, and the resulting protein model was used as the receptor

model in the studies. The 26 structures with experimental determine activities (Kd data) are shown in Table 1. Ligprep module incorporated in Phase was used to prepare the compounds, and compute of the probable ionization state at pH  $7.4 \pm 0.2$ . Phase 3.0 package was used to generate the pharmacophore for CDK2 inhibitors. Desmond was used to performed the molecular dynamic study using OPLS\_2005 force field. The prepared structures were used to generate a pharmacophore model using their biological activity measured in Nm. Ligands were set as active

The data set was divided in a training and test set, respectively, considering a uniform distribution of Kd values in training and test sets. The pharmacophore of these compounds was rationalized from a set of six pharmacophore characteristics: negatively charged group (N) positively charged group (P) and aromatic ring (R) hydrogen bond acceptor (A), hydrogen bond donor (D), hydrophobic group (H). Each pharmacophore feature was defined by a set of chemical structure characteristics. Pharmacophore was explain by the type, location and directionality of each component [15]. Several pharmacophore hypothesis were generated. The hypotheses were ranked according to the following scores: alignment, vector score and a volume score respectively. The predictive power of the QSAR model was validated by the test set compounds externally and internally. Chemical space of activity was also represented in parallel for the observed dissociation constant (Kd) and predicted dissociation constant (Kdp). Balaban index [16], total valence connectivity, Log P and polar surface area (PSA) were used to generate a 3D wire frame surface plot.

Two compounds were chosen for a comparative study: (i) the compound with the best experimentally determine Kd and (ii) Staurosporine. Conformational analysis of the two molecules together with low molecular dynamics applied to CDK2 complex with the compounds was performed. Conformational analysis was used to characterize the regions of the compound exposed to the solvent and present high mobility comparative with the rest of the molecule. In this respect, by rotating the atoms residue around the molecule with 1 degree of freedom,  $-180 + 180$  degrees, a graph containing conformational energies of the structure is obtained. This graph is used to make assumptions regarding compound binding. Low molecular dynamic [17,18] is a technique for observing discrete changes in structure of proteins especially regarding the residues present in binding sites. In this technique, a molecular dynamic is performed on a molecule having the amino acids of the active zone fully flexible, the neighboring residues fixed and distant residues being inert. Two steps were adopted: (i) molecular 3D-similarity indices were computed (for the 26 structures whose activity had been experimentally reported in Table 1) in view of 3D-QSAR study; (ii) docking and molecular dynamics (MD) simulation were performed in order to explore favorable coordinates of the CDK2 inhibitors in docking as well as to understand the large variation in the binding affinities of those compounds with CDK2.

## Results

20 hypotheses were produced and analyzed. After analyzing active ligands alignment and the generated hypotheses, hypothesis AADRR19 was selected. The selected hypothesis contained one hydrogen bond donor (D4), two hydrogen bond acceptors (A2 and A3), and two aromatic rings (R10 and R12), as shown in Figure 1.

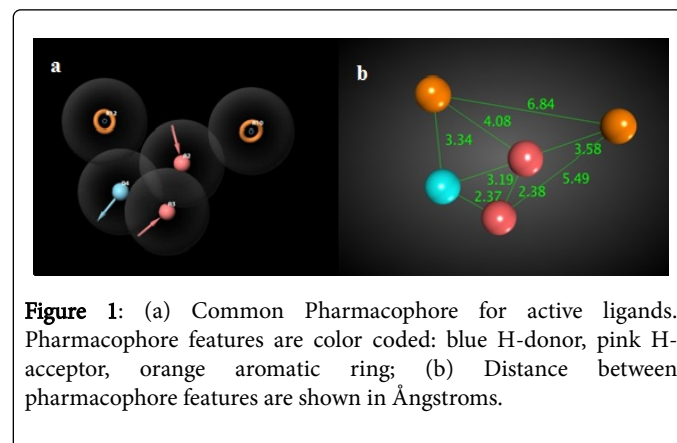


**Figure 1:** (a) Common Pharmacophore for active ligands. Pharmacophore features are color coded: blue H-donor, pink H-acceptor, orange aromatic ring; (b) Distance between pharmacophore features are shown in Ångstroms.

QSAR, obtained independently of pharmacophore model generated using Schrodinger software, has the following statistical parameters: The training set Pearson  $R^2=0.9838$ , with a mean standard error  $MSE=0.446$  (see the plot in Figure 2). Descriptors that have high impact on model building were PSA of compounds followed by potential energy of the compounds and AlogP respectively. Topological descriptors used have a modest contribution to the model. From all MW and polarity had the modest contribution in model architecture. General model equation  $y=0.8674x+270.92$  where  $y$  is the target variable,  $x$  a certain dependent variable.

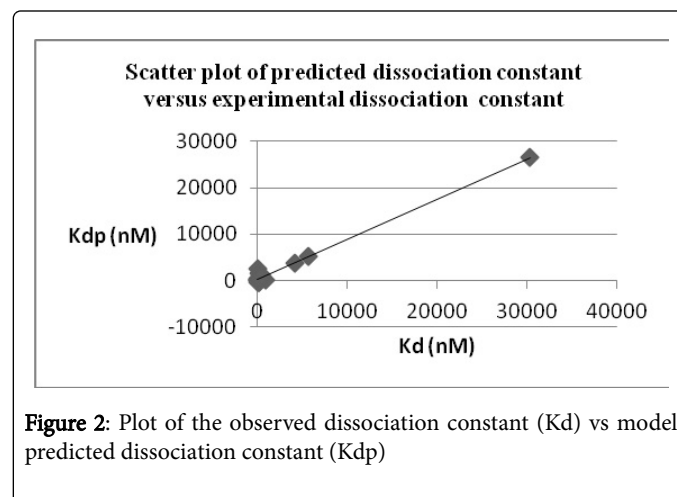


**Figure 2:** Plot of the observed dissociation constant (Kd) vs model predicted dissociation constant (Kdp)

Kd	MW	AlogP	PSA	MR	P	ZM1	W	Xu	Ram	GMT	ECC	PE
MW		0.862	0.9	0.976	0.973	0.977	0.963	0.981	0.922	0.978	0.978	0.28
AlogP	0.862		0.604	0.821	0.844	0.856	0.828	0.808	0.908	0.834	0.755	0.42
PSA	0.9	0.604		0.89	0.839	0.83	0.916	0.894	0.712	0.917	0.963	0.12

MR	0.976	0.821	0.89		0.985	0.96	0.93	0.994	0.844	0.938	0.969	0.18
P	0.973	0.844	0.839	0.985		0.99	0.893	0.993	0.896	0.915	0.94	0.24
ZM1	0.977	0.856	0.83	0.96	0.99		0.894	0.979	0.943	0.924	0.0.932	0.32
W	0.963	0.828	0.916	0.93	0.893	0.894		0.92	0.848	0.995	0.968	0.25
Xu	0.981	0.808	0.894	0.994	0.993	0.979	0.92		0.871	0.937	0.971	0.21
Ram	0.922	0.908	0.712	0.844	0.896	0.943	0.848	0.871		0.883	0.83	0.53
GMT	0.978	0.834	0.917	0.938	0.915	0.924	0.995	0.937	0.883		0.976	0.28
ECC	0.975	0.755	0.963	0.969	0.94	0.932	0.968	0.971	0.83	0.976		0.19
PE	0.282	0.419	0.122	0.178	0.242	0.315	0.25	0.209	0.53	0.28	0.2	

**Table 1:** Descriptors correlation matrix: Kd-dissociation constant (nM), MW-molecular weight, AlogP-partition constant, PSA-polar surface area, P-polarity, ZM1-first Zagreb index, W-Wiener index, Xu-Xu index, Ram -ramification index, GMT1-Gutman molecular topological descriptor1, ECC-Eccentricity, PE-potential energy.

Discret equation of descriptors for the target variable (y) correlation  $y = PE^*0.00234096 + 0.11584$ ,  $y = MW^*0.00252934 - 0.388785$ ,  $y = AlogP^*0.178285 + 0.128918$ ,  $y = PSA^*0.00655576 - 0.278792$ ,  $y = MR^*0.0101536 - 0.457824$ ,  $y = P^*0.020245 - 0.361666$ ,  $y = ZM1^*0.00655738 - 0.359016$ ,  $y = W^*0.000183697 + 0.0461768$ ,  $y = Xu^*0.0411207 - 0.471759$ ,  $y = GMT^*4.16536e-05 + 0.0495158$ ,  $y = ECC^*0.00186047 - 0.0469767$ .

Predicted activities of the observed and test set molecules are also listed in Table 2.

	Molecule	Kd	Kdp	Lipinski rule of 5
1	<chem>O=C(C1=CC=C(C(O)=O)C=C1)NC(=C2)NN=C2C3CC3</chem>	5600	5300.54	271.096; 4; 3; 5; 2.18
2	<chem>O=S(=O)(NCC[NH](C)C)C(=CC=1)C=CC=1N=CC2C=3C=CC=CC=3NC2=O</chem>	840	61.653	386.141; 5; 2; 7; -0.087
3	<chem>O=C1NC2=CC=C3N=CSC3=C2C1C=NC(=CC=4)C=CC=4S(=O)(O)=NC(=O)C</chem>	194	539.074	414.046; 5; 2; 4; -0.942
4	<chem>O=C1NC2=CC=C3N=CSC3=C2C1C=NC(=CC=4)C=CC=4S(=O)(=O)NC=5C(OC)=CC=CC=5OC</chem>	179	65.1354	508.088; 7; 2; 7; 1.833
5	<chem>O=C1NC2=CC=C3N=CSC3=C2C1C=NC=4C=C5CS(=O)(=O)CC5=CC=4</chem>	36	193.489	383.04; 5; 1; 2; -1.044
6	<chem>O=C1NC=2C=CC=CC=2C1C=NC(=CC=3)C=CC=3S(=O)(=O)NC(=N)N</chem>	210	1240.24	357.09; 6; 4; 5; -1.729
7	<chem>O=C1NC=2C=CC(C(=O)OCC(C)C)=CC=2C1=NNC(=CC=3)C=CC=3S(=O)(N)=O</chem>	47	95.4378	416.115; 6; 3; 7; 2.055
8	<chem>O=C(NC=1NN=C(C2CC2)C=1)CC(=CC=3)C=CC=3OCC[NH]4CCCC4</chem>	44	-331.264	354.206; 5; 2; 9; 2.986
9	<chem>O=C1NC=2C=CC(C(=O)O)=CC=2C1=NNC(=CC=3)C=CC=3S(=O)(N)=O</chem>	8	2445.64	360.053; 6; 4; 4; 0.372
10	<chem>NC(S1)=NC(C)=C1C(N=2)=CC=NC=2NC(=CC=3)C=CC=3N(C)C</chem>	190	48.7439	326.131; 6; 2; 4; 3.222
11	<chem>C1C(=C1)C(N(C)C)=CC=C1NC(=N2)N=CC=C2C=3SC(C)=NC=3C</chem>	45	323.486	359.097; 5; 1; 4; 4.732
12	<chem>O=N(O)C(C=1)=C(N(C)C)C=CC=1NC(N=2)=NC=CC=2C=3SC(C)=NC=3C</chem>	62	13.1525	371.129; 6; 2; 5; 0.656
13	<chem>N#CC(=C1)C=CC=C1NC(=N2)N=CC=C2C=3SC(C)=NC=3C</chem>	161	56.4688	307.089; 5; 1; 4; 3.285
14	<chem>O=N(O)C(C=1)=CC=CC=1NC(N=2)=NC=CC=2C(S3)=C(C)N=C3NCC=C</chem>	54	2.1458	369.113; 6; 3; 7; 1.345
15	<chem>O=N(O)C(C=1)=CC=CC=1NC(N=2)=NC=CC=2C=3SC(C)=NC=3C</chem>	73	288.23	328.087; 5; 2; 4; 0.491
16	<chem>FC(=CC=1)C=CC=1NC(=N2)N=CC=C2C=3SC(C)=NC=3C</chem>	121	-399.515	300.084; 5; 1; 3; 3.946
17	<chem>C1C(=CC=1)C=CC=1NC(=N2)N=CC=C2C=3SC(C)=NC=3C</chem>	151	-403.74	316.055; 4; 1; 3; 4.516
18	<chem>O=C1NC2=CC=C3NNN=C3C2=C1N=NC(=CC=4)C=CC=4S(=O)(=O)N</chem>	191	1667.32	357.064; 8; 4; 3; -0.995

19	<chem>O=C(N1)C(=NNC2=CC=C(S(=O)(N)=O)C=C2)C(C=3)=C1C=CC=3C(=O)NCC4=C(OC)C=CC=C4OC</chem>	23	79.8934	509.137; 8; 4; 9; 1.324
20	<chem>O=C1NC=2C=CC(C(NCCC3=CN=CN3)=O)=CC=2C1=NNC(=CC=4)C=CC=4S(=O)(=O)N</chem>	251	241.264	453.122; 8; 5; 8; -0.956
21	<chem>O=C(NC1=CC(C2CC2)=NN1)CC(=CC=3)C=CC=3C=4SC=CC=4</chem>	79	351.827	323.109; 3; 2; 6; 4.267
22	<chem>FC(F)(F)OC(=CC=1)C=CC=1CC(=O)NC(=C2)NN=C2C3CC3</chem>	463	766.564	325.104; 7; 2; 7; 3.321
23	<chem>BrC(C=C1)=CC=C1C(=O)NC(=C2)NN=C2C</chem>	4090	3833.97	279.001; 3; 2; 3; 2.734
24	<chem>O=C(C1=CC=C(C(N)=O)C=C1)NC(=C2)NN=C2C3CC3</chem>	362	1456.82	270.112; 4; 3; 5; 1.03
25	<chem>O=C(CCC)NC(C=1)=NNC=1C2CC2</chem>	360	854.64	193.122; 3; 2; 5; 1.813
26	<chem>NC(=N1)N=CC=C1C=2SC(C)=NC=2C</chem>	30300	26533.1	206.063; 4; 1; 1; 1.129

**Table 2:** Molecules used in building QSAR model for CDK2 inhibitors. Smiles, Dissociation constant Kd (in nM), predicted dissociation constant Kdp (in nM) and Lipinski's rule of five (from left to right): molecular mass in Daltons, number of H donor groups, number of H accepting groups, number of rotatable bounds, and octanol-water partition coefficient.

As shown in Figure 1, the presence of two H-acceptor groups, two aromatic rings and one H-donor group is mandatory for the inhibitory effect on CDK2. By superimposing the common pharmacophore model on the best hit (compound #9) one observes that both coordinations of H-acceptor groups are the same. Also by superimposing the best hit #9 over #26, with the lowest Kd, one observes that #9 has six H acceptor groups, four H-donor groups, two hydrophobic groups and two hydrogen bond forming groups,

compared with three H acceptor groups, two H donor groups, two hydrophobic groups, and two aromatic groups, for #26. By increasing the number of H acceptor groups and the distance between hydrophobic and aromatic groups, larger Kd values are observed. Also orientation/alignment of ligand in the binding site is crucial. Figure 3 illustrates superposition of #9 over the common pharmacophore comparative to #26; one observes a difference of 90o between orientation of #9 and #26, respectively.

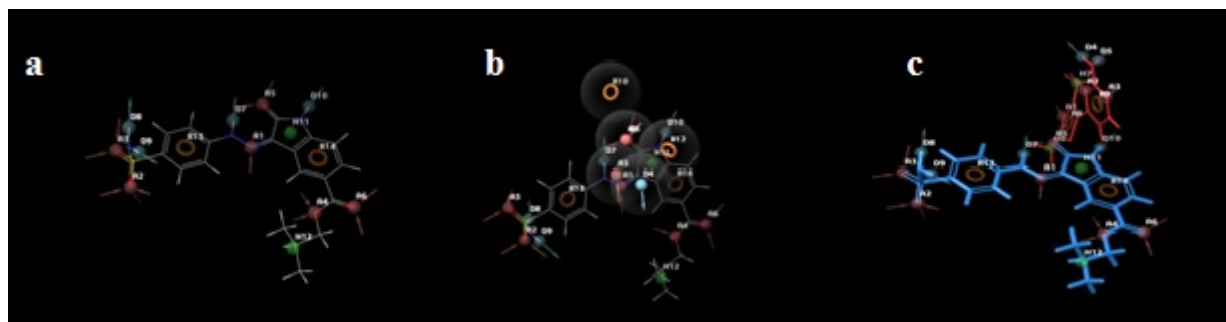


**Figure 3:** (a) Ligand 9 with H acceptor groups in pink, H-donor groups in blue, aromatic rings in orange and hydrogen bond forming groups in green; (b) ligand 9 superimposed with the commonest pharmacophore; (c) ligand 9 in blue superimposed with ligand 26 in red.

Chemical space of activity, represented in topological terms, showed similar coordinates for Kd and Kdp (represented using Balaban index, a highly discriminating index) and total valence connectivity. Chemical space of drug like properties represented using polar surface area and Log P shows the same shape as the topological space (Figures 4 and 5).

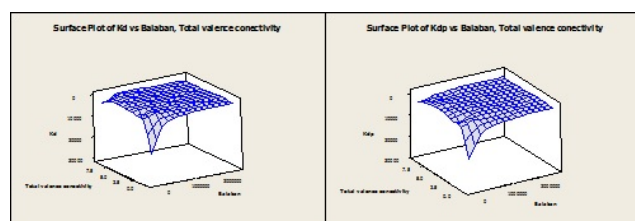


**Figure 4:** Surface plots of dissociation constant, experimental (Kd) left and predicted (Kdp) right, vs Balaban index and total valence connectivity.

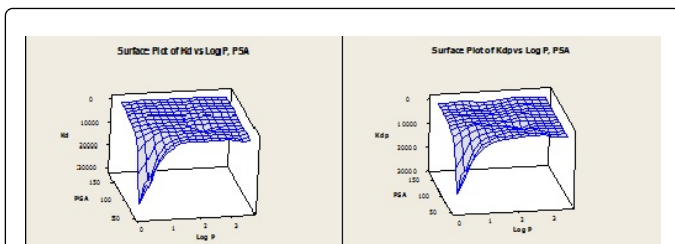


**Figure 5:** Surface plots of dissociation constant, experimental (Kd) and predicted (Kdp) vs polar surface area (PSA) and Log P.

Compound #9 in complex with CDK2 was compared with the crystallographic structure of the CDK2 complex with inhibitor Staurosporine.

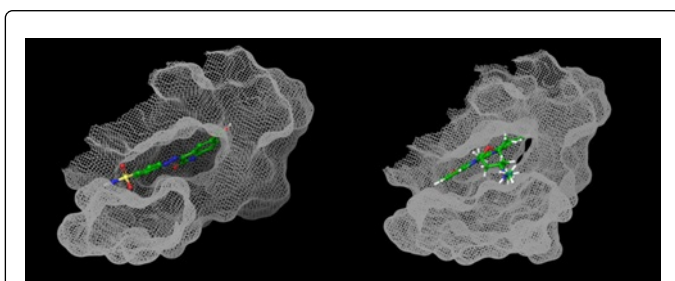


**Figure 6:** a Compound #9 (left) and b Staurosporine (right) in CDK2 binding pocket; binding pocket configuration of #9 was obtained by docking it with CDK 2 structure, retrieved from 1QA1 using the same binding site; best rank pose is represented. Staustosporin in complex with CDK2 was imported from 1AQ1 PDB model.

Compound #9 forms (by giving away a proton from N 4582 with  $\pi$  electrons from Phe 80) an aren-H bond, O 4602 accepts a proton from Gln 85 and forms an H-bond, N4603 gives away a proton and forms with Leu 83 an H-bond. Then O4588, C4534, C 4544, C4549, O 4602 and O4604 respectively are exposed to the solvent. Staurosporine orientation in CDK2 binding pocket N2252 donates a proton and forms with Glu 81 an H-bond, O2254 accepts a proton and forms with Leu 83 an H-bond, O2231 accepts a proton from Gly 11 and forms an H-bond. The protonated N 2264 from NH2 group gives two protons and forms H-bonds with Asp 86 and Gln 131 and also by its positive charge forms a salt bridge with Asp 86, N2264 and its bond C2205 are highly exposed to the solvent; also C2235, C2233, C2257, C2258 are exposed to the solvent. Furthermore, it is observed that both structures are aligned coplanar in the binding pocket. Both compounds have an external hook highly exposed to solvent that keeps the compounds in the binding pocket. Regarding # 9 the hook is represented by the sulfonic amide group while in case of Staurosporine by the methylated N2264 (Figure 6).

By superimposing # 9 with Staurosporine (Figure 7), one observes that difference in activity and consecutively in specificity is given by the regions exposed to the solvent and form close bonds with the amino acids present at the margin of the binding pocket. Conformational analysis of these regions for both compounds showed that: (i) in case of Staurosporin the ramified exposed residues, when rotated around the binding pocket, have significantly favorable

energies compared with the hooked regions of # 9 that has higher conformational energies. It is observed that Staurosporin has lower energy values and a large energy domain in contrast with # 9. Regions with lower conformational energies suggest a stronger binding and a larger topological domain for forming favorable bonds. Some conformational energy values are shown in Figure 8 (see supplemental material for C(2265)-N(2264)-C(2234)-C(2233); O(3957)-S(3956)-C(3955)-C(3952); O(3957)-S(3956)-N(3958)-H(3970).

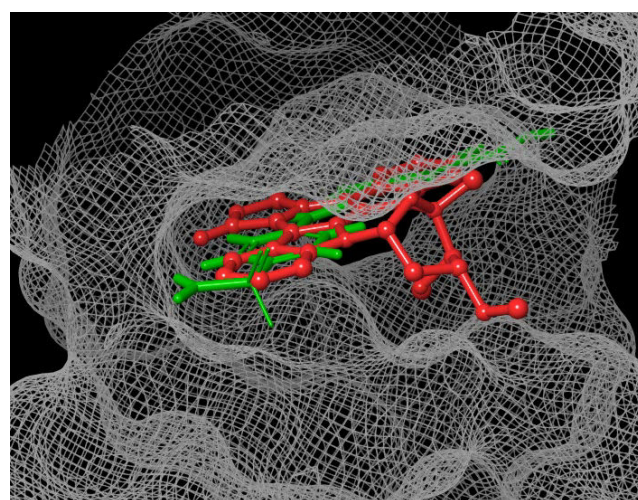


**Figure 7:** Staurosporine (red) superimposed to # 9 (green).

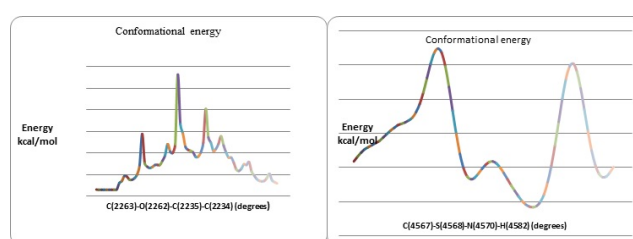
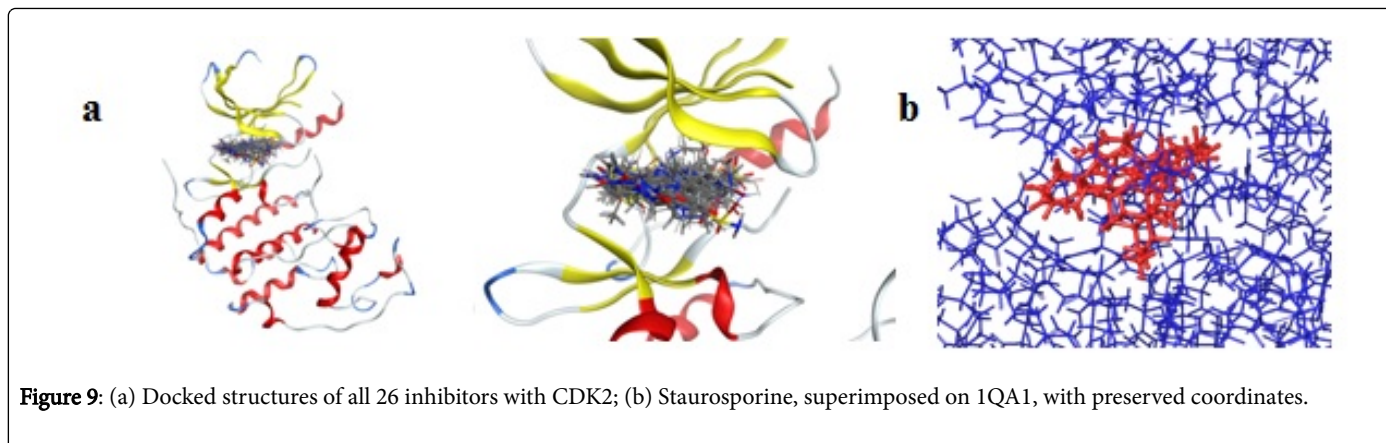
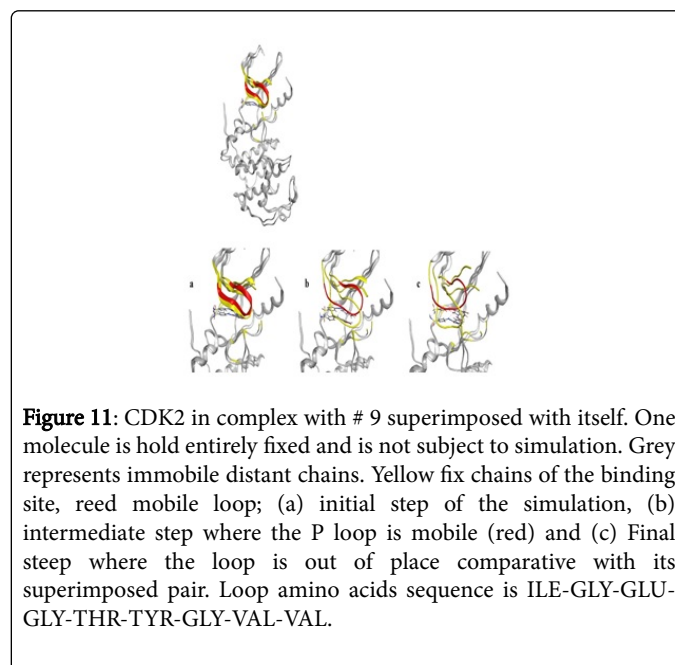
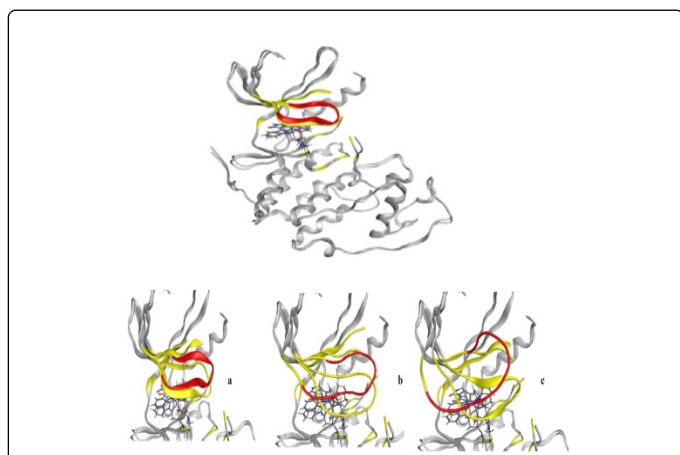


**Figure 8:** Conformational energy for residue C2263-O2262-C2235-C2234 of Staurosporine (left) and conformational energy of residue C4567-S4568-N4570-H4582 of # 9.

Figure 9a shows all the 26 inhibitors docked into the pocket of CDK2. All molecules were positioned relatively the same, shared a similar binding mode excepting some molecules due to low activity with unfavorable conformations (i.e orientation of the functional groups) for the binding. The binding modes of the most active compounds correspond with the binding mode of the prototype molecule Staurosporine. Compounds with poor activity (see Figure 3) bind differently from Staurosporine. This difference in the binding modes resulted in distinct activities. Molecular docking and dynamics Simulation were done to further characterized the binding mode of the most important functional groups to CDK2. In docking procedure ligands was treated as flexibly and the protein was held fixed. RMSD value for heavy atoms of the ligands, between the generated docked pose and the native pose was 0.82 Å (Figure 9a). Docking was able to reproduce the native conformation successfully (low RMSD value between the docked pose and the initial geometry) (Figure 9b).



Low molecular dynamic applied on CDK2 complex with a ligand 9 and Staurosporine, respectively, demonstrated the presence of P loop. Target temperature was set to be 310.15Ko. The final model (Figures 10a-c and 11) was retrieved after 9 picoseconds. One structure was maintained inert for analogy with second structure on which low molecular dynamics was applied. All operations were made on the minimized second structure.



In summary a strategy based on multiple computation techniques was used in order to explore the structure base inhibition process for a series of CDK2 inhibitors. Docking was utilized to generate hypothetical binding modes for ligands. Low molecular dynamic was used to evaluate the binding mode from the receptor perspective. Both Staurosporine and #9 have a lipophilic core made of coplanar aromatic rings that fit into the binding pocket. As suggested by the QSAR model shape is of curtail importance. Both Staurosporine and #9 have an external region that binds with marginal amino acids acting like a “hook” in fixing the compound at it’s site. Furthermore the satisfactory agreement between experiment and theory and between QSAR model and pharmacophore model (build independently) suggested that the QSAR model has good correlation and predictive power and straitens suggested findings.

## References

1. Chae HJ, Kang JS, Byun JO, Han KS, Kim DU, et al. (2000) "Molecular mechanism of staurosporine-induced apoptosis in osteoblasts", *Pharmacol Res* 42: 373-381.

2. Eaton BE, Gold L, Zichi DA (1995) Let's get specific: the relationship between specificity and affinity. *Chem & bio* 2: 633-638.
3. Elmore S (2007) Apoptosis: A Review of Programmed Cell Death, *Toxicol Pathol* 35: 495-516.
4. Liu T, Lin Y, Wen X, Jorrisen RN, Gilson MK (2007) A web-accessible database of experimentally determined protein-ligand binding affinities *Nucleic Acids Res* 35: 198-201.
5. Pierce MM, Raman CS, Nall BT (1999) Isothermal titration calorimetry of protein-protein interactions. *Methods* 19: 213-21.
6. Walker JE, Saraste M, Runswick MJ, Gay NJ (1982) Distantly related sequences in the alpha- and beta-subunits of ATP synthase, myosin, kinases and other ATP-requiring enzymes and a common nucleotide binding fold, *EMBO J* 1: 945-951.
7. Khalifeh MH, Yousefi-Azari H, Ashrafi AR (2009) The first and second Zagreb indices of some graph operations. *Dis App Math* 157: 804-811.
8. Wiener H (1947) Structural determination of paraffin boiling points, *J Am Chem* 69: 17-20.
9. Doucet JP, Panaye A (2010) Three dimensional QSAR: applications in pharmacology and toxicology. CRC Press: pp: 212-213.
10. Sheeba Agnes V (2015) Degree distance and Gutman index of corona product of graphs. *Transactions on Combinatorics* 4: 11-23.
11. Devillers J, Balaban AT (1999) editors. Topological indices and related descriptors in QSAR and QSPAR. CRC Press: pp: 65-66.
12. Lipinski CA, Lombardo F, Dominy BW, Feeney PJ (2001) Experimental and computational approaches to estimate solubility and permeability in drug discovery and development settings, *Adv Drug Deliv* 46: 3-26.
13. Morris GM, Huey R, Lindstrom W, Sanner MF, Belew RK, et al. (2009) AutoDock4 and AutoDockTools4: Automated docking with selective receptor flexibility. *J comp chem* 30: 2785-91.
14. Lawrie AM, Noble ME, Tunnah P, Brown NR, Johnson LN, et al. (1997) Protein kinase inhibition by staurosporine revealed in details of the molecular interaction with CDK2. *Nat stru biol* 4: 796-801.
15. Dixon SL, Smondyrev AM, Knoll EH, Rao SN, Shaw DE, et al. (2006) PHASE: a new engine for pharmacophore perception, 3D QSAR model development, and 3D database screening: 1. Methodology and preliminary results. *J com-aided mol des* 20: 647-671.
16. Balaban AT (1982) Highly Discriminating Distance-based Topological Index. *Chem Phys Lett* 89: 399-404.
17. Godha K, Hakoshima T (2008) A molecular mechanism of P-loop pliability of Rho-kinase investigated by molecular dynamic simulation. *J Comp-Aided Mol Des* 22: 789-797.
18. Labute P (2010) LowModeMD-Implicit Low-Mode Velocity Filtering Applied to Conformational Search of Macrocycles and Protein Loops. *J Chem Info Mod* 50: 792-800.